

1 **Single crystalline superstructured stable single**

2 **domain magnetite nanoparticles**

3
4 Victoria Reichel, András Kovács, Monika Kumari, Éva Bereczk-Tompa, Emanuel Schneck, Patrick
5 Diehle, Mihály Pósfai, Ann M. Hirt, Martial Duchamp, Rafal E. Dunin-Borkowski and Damien Faivre

6 7 **Supporting Information**

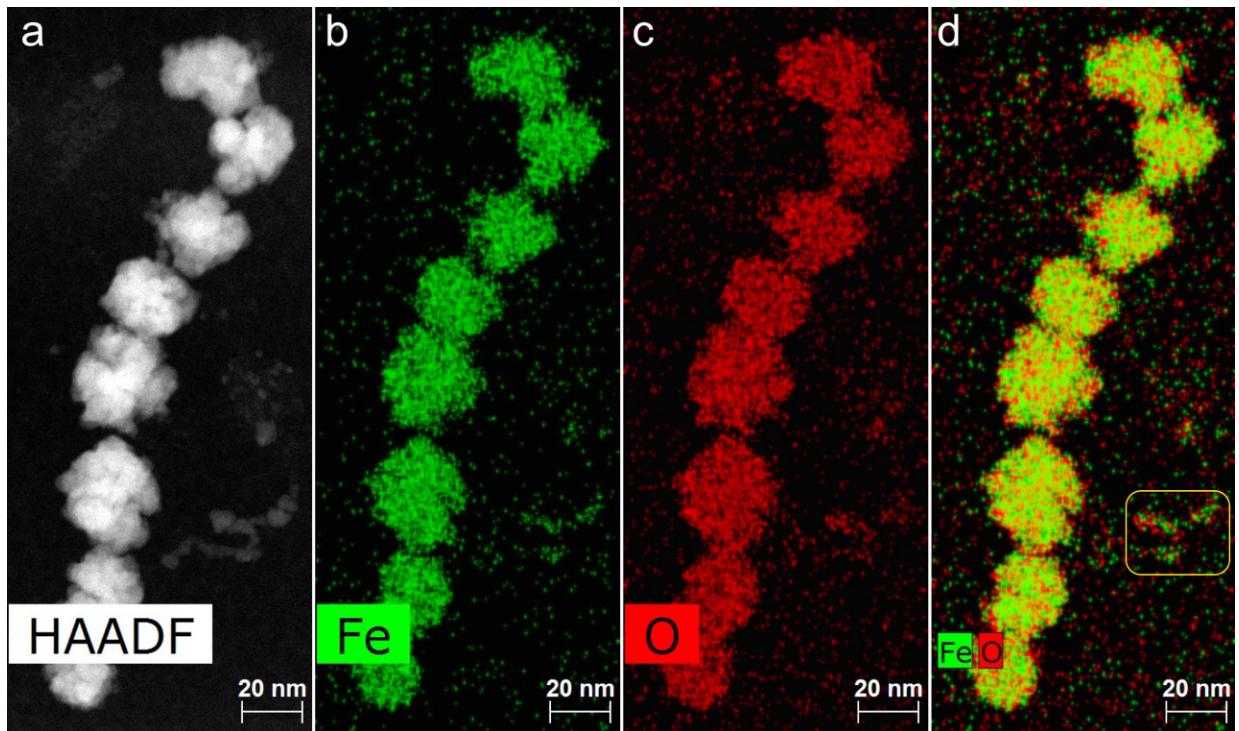
8 **Supporting characterization**

9 The magnetite particles are, as expected, composed of Fe and O, as measured by energy-
10 dispersive X-ray spectroscopy (EDXS) (Fig. S1). In addition to the signals from the 40 nm
11 particles, Fe and O signals are also recorded from smaller particles that are dispersed on the
12 TEM grid (boxed area to the right of the lower part of the magnetite chain in Fig. S1d). These
13 smaller features may represent the precursor iron oxide particles that first form during the
14 synthesis process. The presence of C in the particles was checked in EDXS maps obtained
15 from parts of the particles that extended above holes in the lacey C support film (without
16 the contribution of a C-containing background, Fig. S2). The inhomogeneous distribution of
17 the C signal observed within the particles (Fig. S2b) suggests that some C is present inside
18 them, perhaps originating from polyarginine; however, the presence of C-bearing
19 contamination arising from interaction between the intense and very small electron probe
20 and the particle surface cannot be excluded. Elemental maps recorded using electron
21 energy-loss spectroscopy (EELS) also confirmed the Fe–O composition of the particles
22 (Fig. S3). From EELS spectrum images, it is also possible to extract information about the

1 relative thickness of the magnetite particles t/λ , where t is the thickness and λ the mean
2 free path of the electrons, by taking the ratio of the integrated intensities of the zero-loss
3 peak and the total EEL spectrum. Such a thickness map is shown in Fig. S3b. A STEM HAADF
4 image clearly shows individual sub-units within two particles (Fig. S4a), and slices extracted
5 from tomographic reconstructions indicate that these sub-units are not fused; instead, gaps
6 occur between them (Fig. S4b). Electron tomographic reconstructions (Fig. S4c,d) show
7 highly irregular surfaces, presumably resulting from the aggregation of sub-units. Selected-
8 area electron diffraction (SAED) patterns obtained from single, aligned particles (Fig. S5) and
9 Fourier transforms of HRTEM images (Fig. S6) reveal that the sub-units within each particle
10 occur in a uniform crystallographic orientation. The sizes of sub-units observed in TEM
11 images are consistent with information extracted from small angle neutron scattering (SANS)
12 (Fig. S7) and bulk magnetic experiments (Fig. S8). According to an analysis of X-ray diffraction
13 patterns, the mesocrystals reach their final sizes after 1 hr of synthesis (Fig. S9).

14

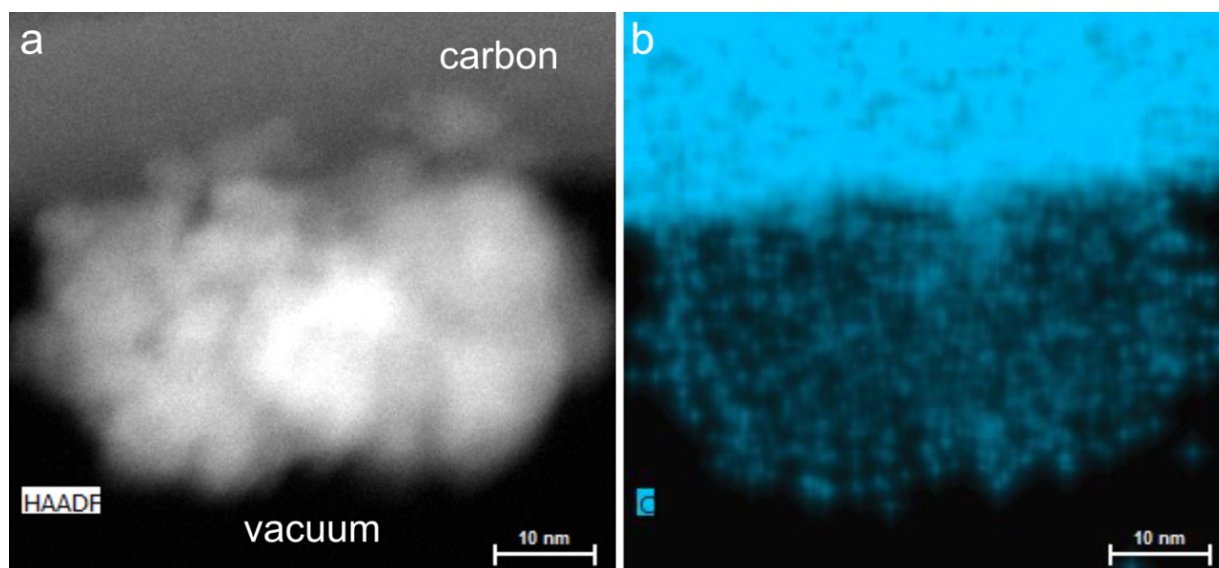
1 **Supporting Figures**



3 Fig. S1: Compositional analysis of a chain of eight magnetite particles. (a) HAADF STEM
4 image; (b) Fe, (c) O, and (d) Fe+O elemental maps obtained from EDXS spectrum images. The
5 boxed area in (d) encloses smaller particles that are also composed of Fe and O.

6

1

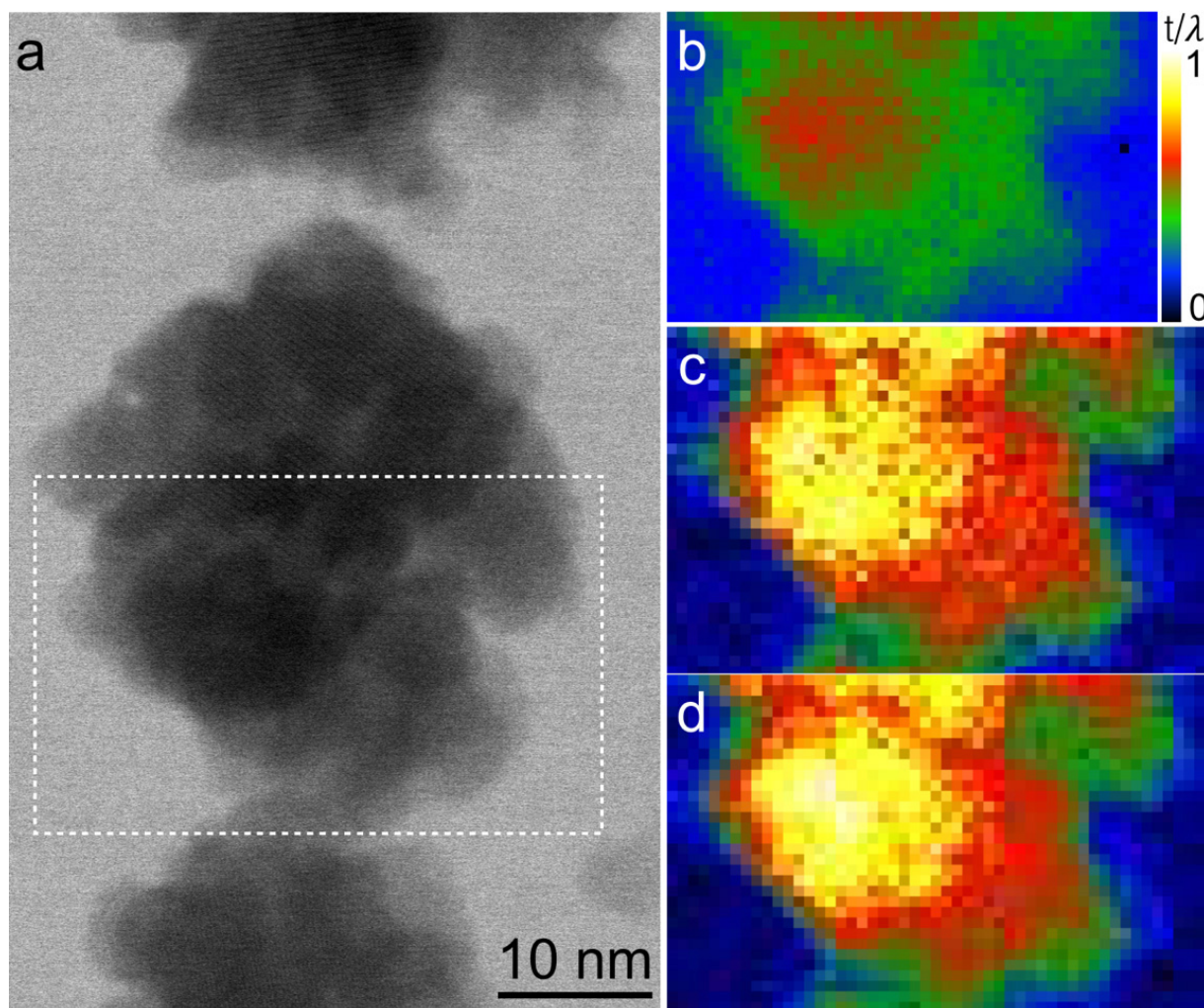


2

3 Fig. S2: Compositional analysis of a single magnetite particle attached to the side of the lacey
4 C support film, with its lower part in vacuum. (a) HAADF STEM image and (b) C elemental
5 map obtained from EDXS spectrum images.

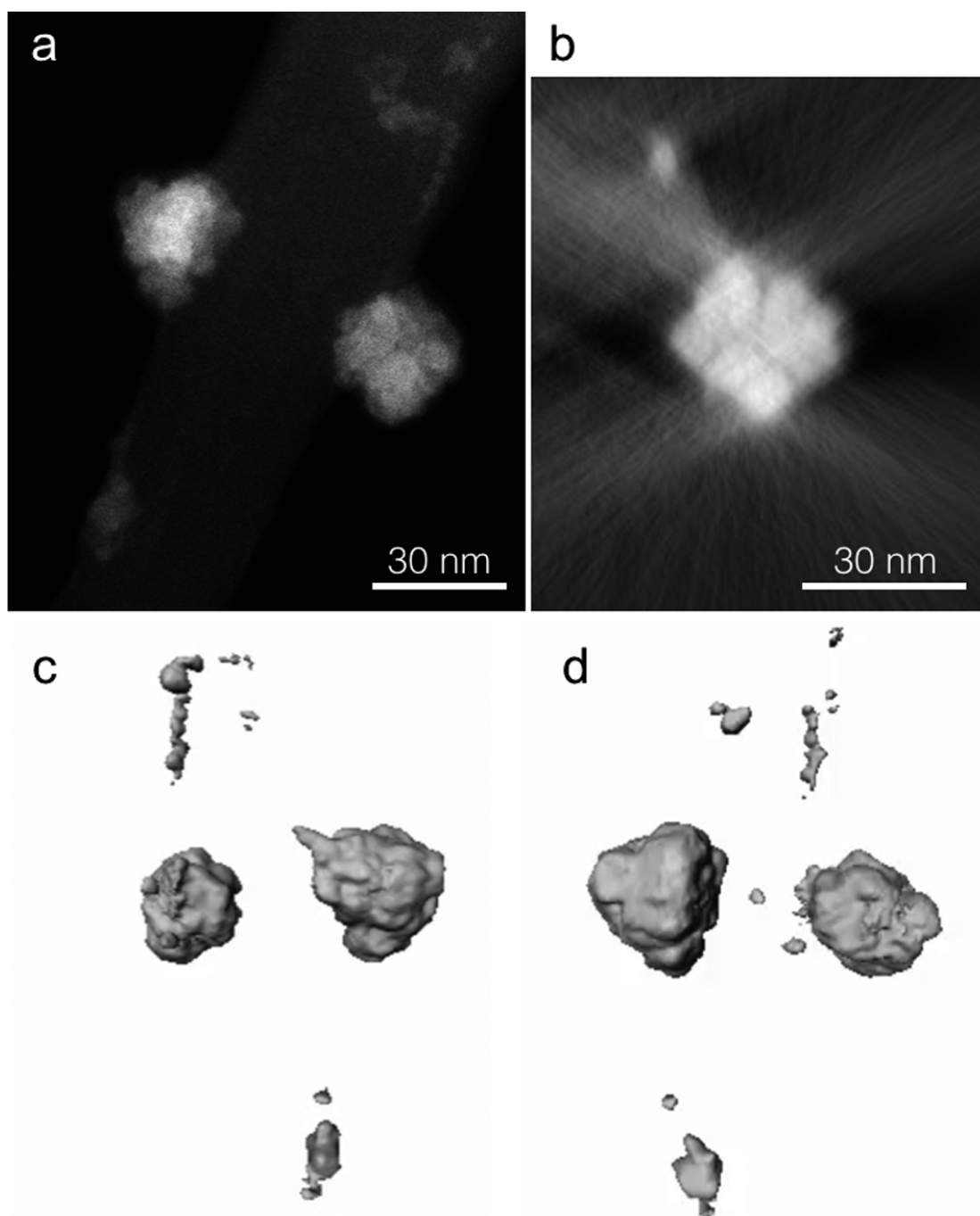
6

1



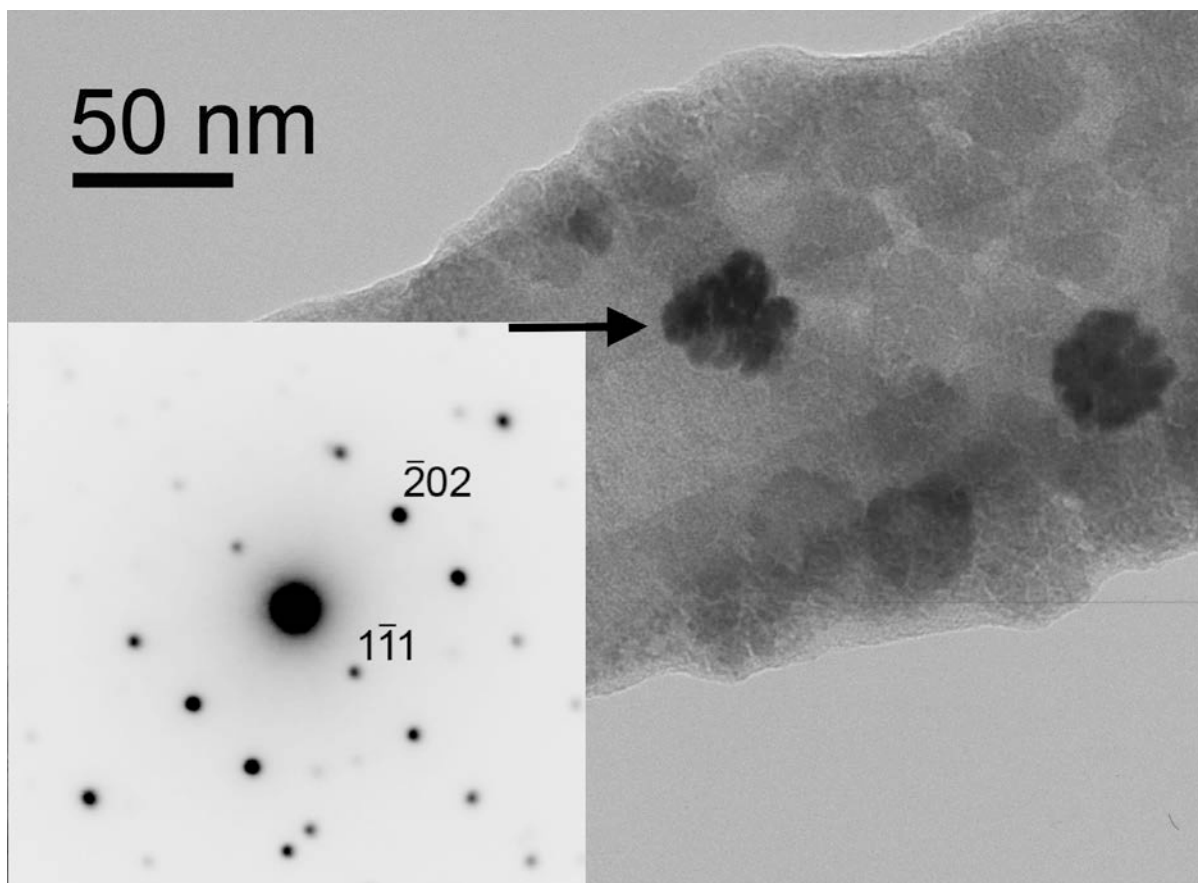
2

3 Fig. S3: Thickness and elemental distribution maps of a magnetite particle derived from a
4 STEM EELS spectrum image. (a) BF STEM image. The area within the rectangle was used for
5 the EELS maps. (b) Relative thickness (t/λ) of the particle. (c) Fe elemental map. (d) O
6 elemental map.

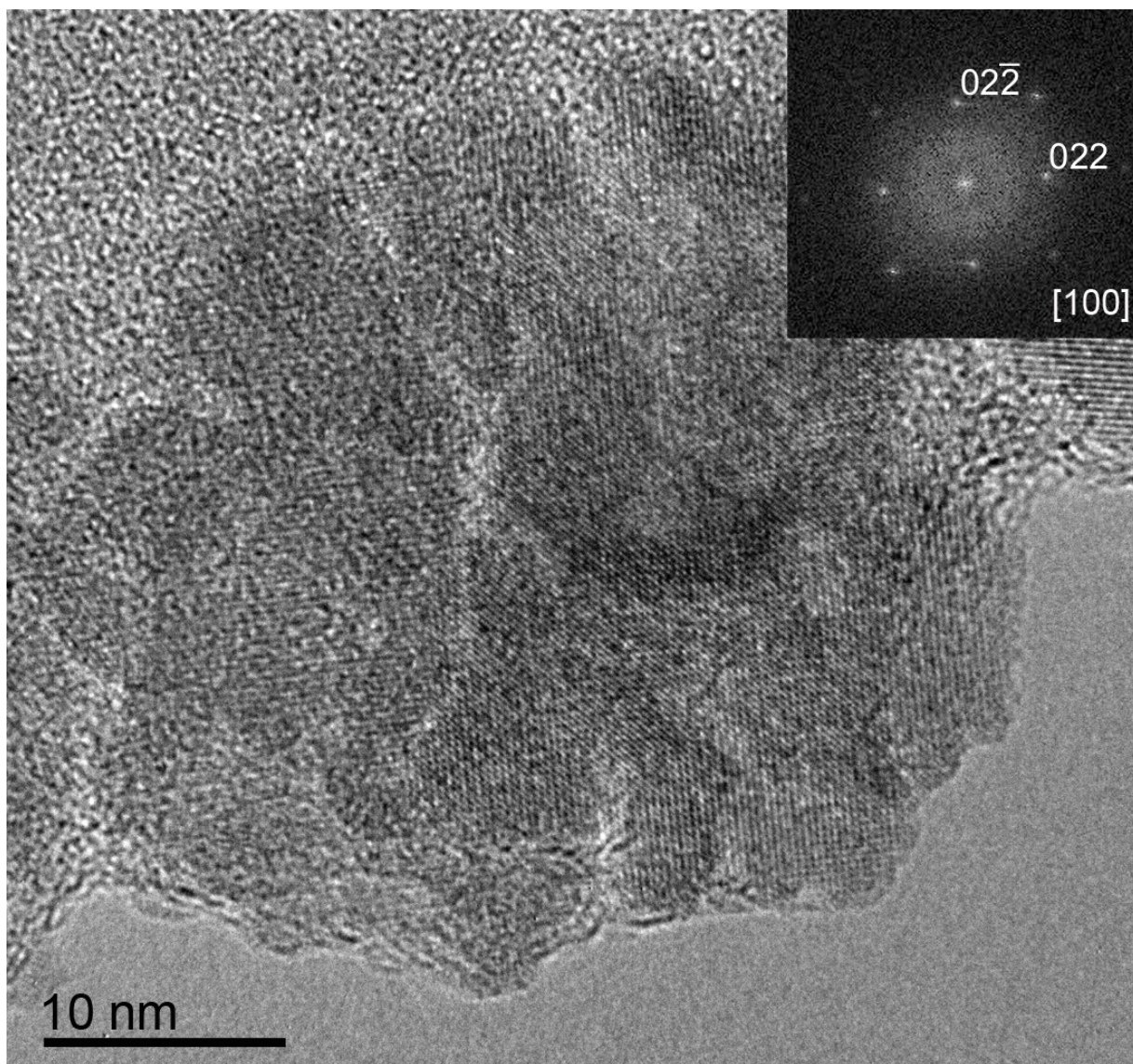


1
2 Fig. S4: (a) HAADF STEM image of two 30-nm particles and several smaller ones on carbon
3 support. (b) Slice of the particle extracted from the tomographic reconstruction showing the
4 ~1-nm-gap between its sub-units. (c,d) Three-dimensional reconstruction of the particles
5 viewed from two different angles.

6

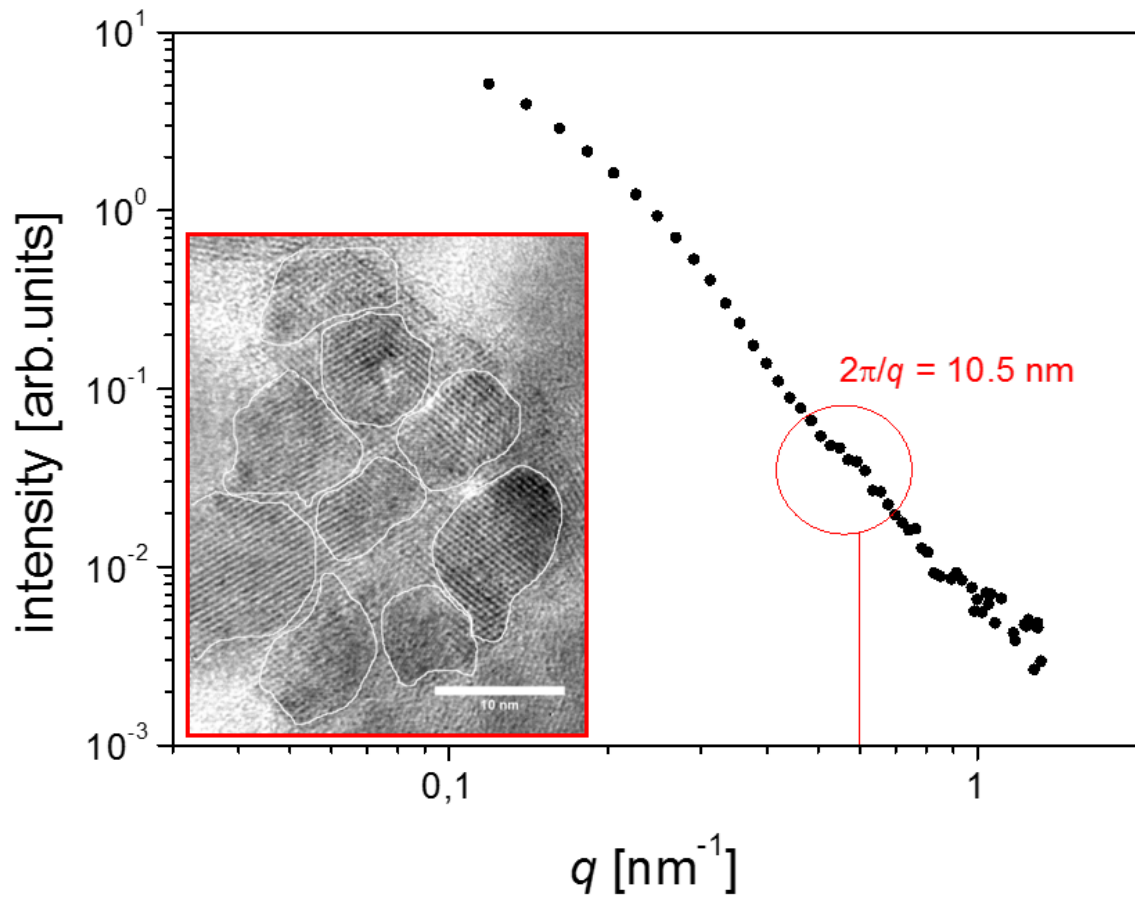


1
2 Fig. S5. Bright-field TEM image of a cluster of magnetite particles on a carbon substrate, with
3 the inset in the lower left showing a single-crystal-like SAED pattern of the arrowed particle,
4 obtained with the electron beam parallel to the $[1\bar{2}1]$ crystallographic direction of
5 magnetite.



1
2
3
4
5
6
7

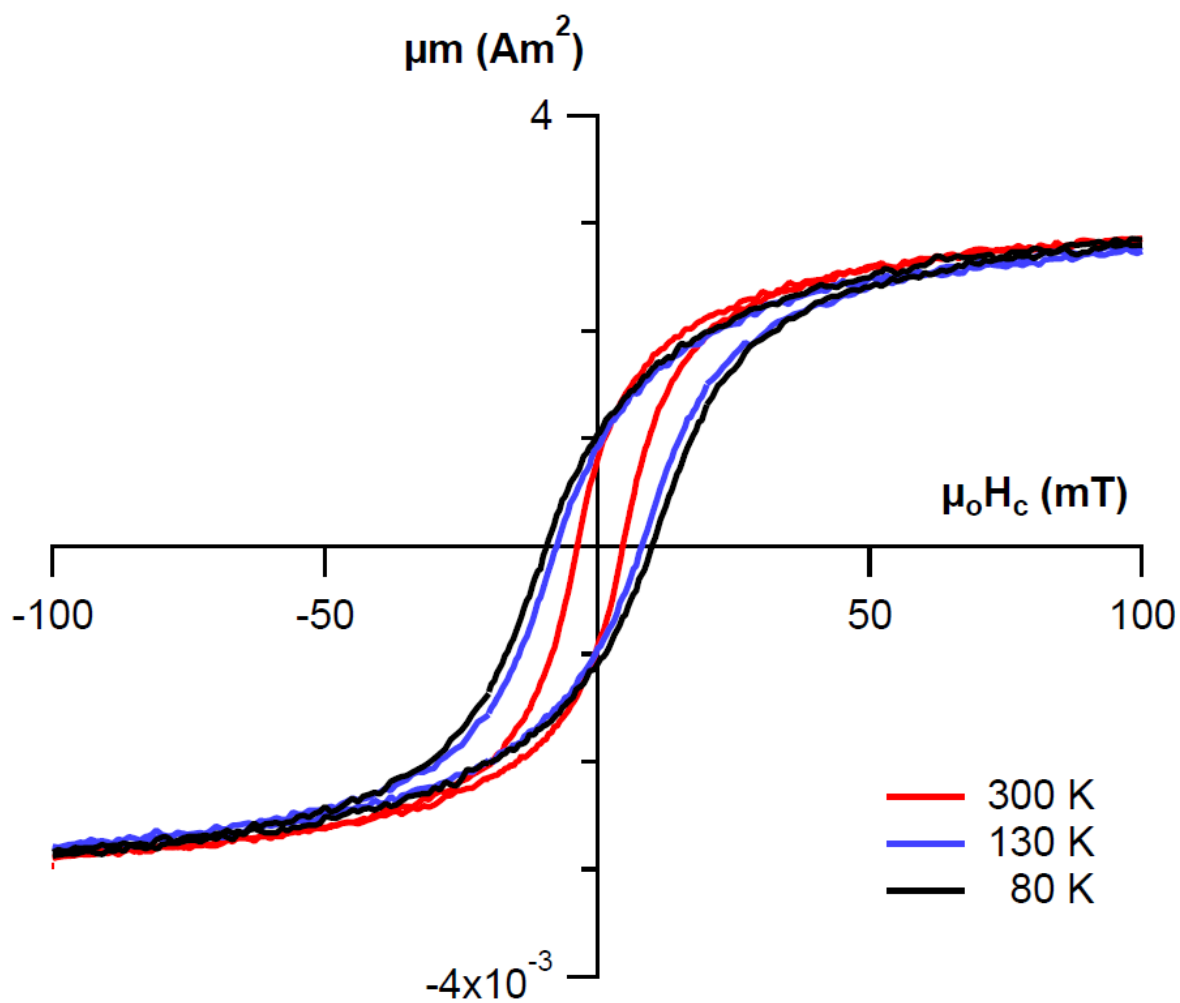
Fig. S6: HRTEM image of a magnetite particle obtained with the electron beam parallel to the $[100]$ direction of magnetite. The Fourier transform of the particle is shown in the inset and indicates that, even though the particle consists of several small crystallites, it is in fact a single crystal. The reflections and the zone axis are indicated in the inset.



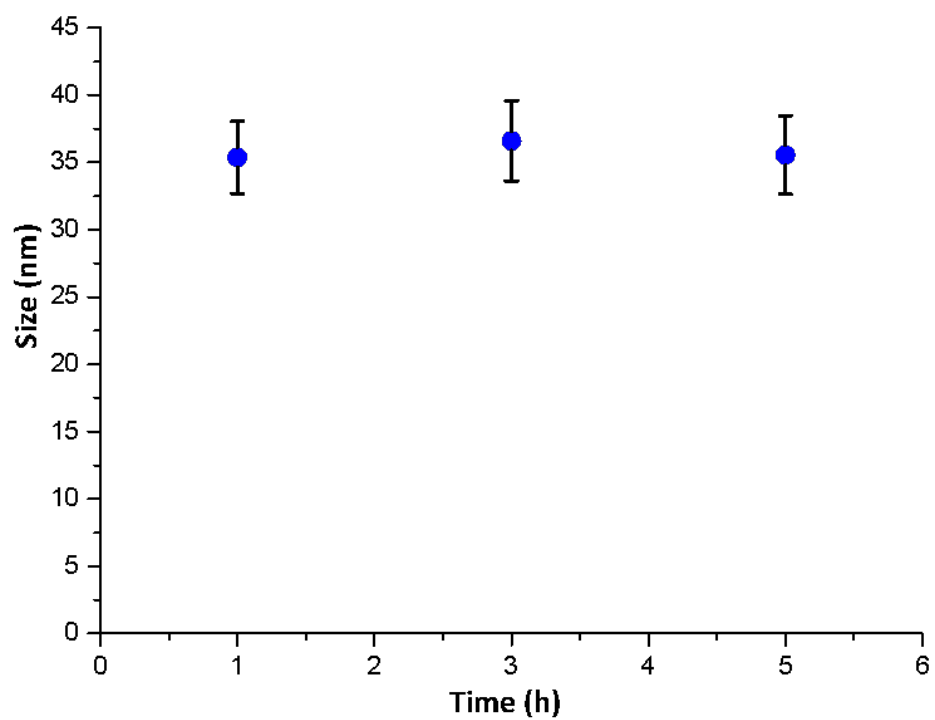
1

2 Fig. S7: Small angle neutron scattering (SANS) curve of magnetite nanoparticles exhibiting a
3 distinct feature around a q value ($\approx 0.6 \text{ nm}^{-1}$) corresponding to a characteristic length scale
4 of 10–11 nm. This length scale is consistent with the average sub-unit size of the magnetite
5 nanoparticles.

6



1
 2 Fig. S8: Temperature-dependent magnetic characterization of the particles. The observed
 3 increase in coercivity at lower temperature is typical for SP particles.
 4

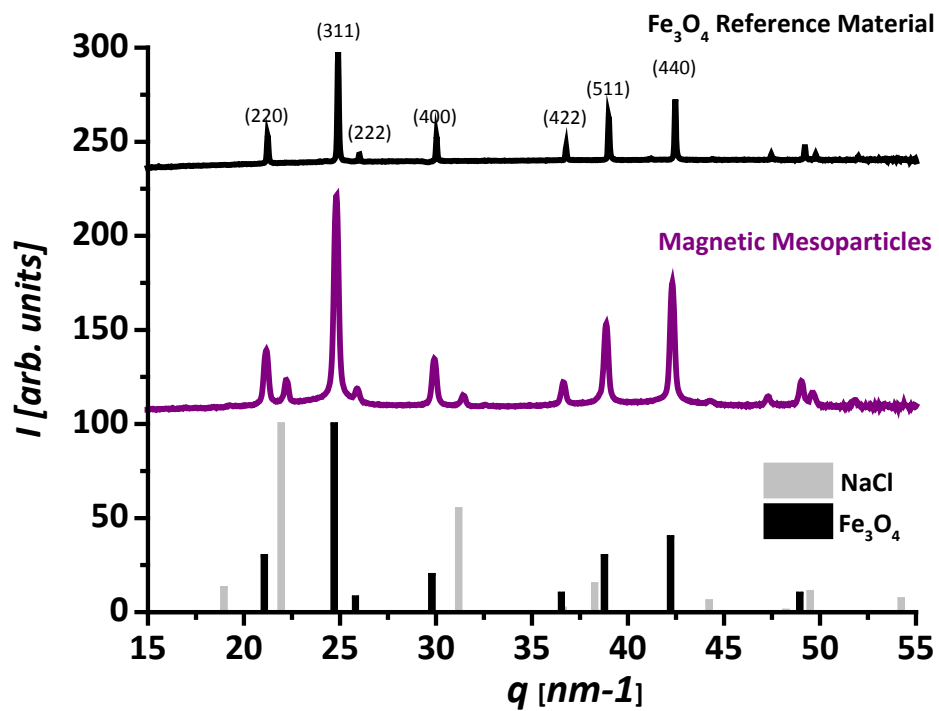


1

2 Fig. S9: Evolution of particle size during synthesis (washed samples after 1h, 3h and 5h of
3 synthesis) as determined by using the Scherrer formula for the most intense magnetite peak
4 in the X-ray diffractogram.

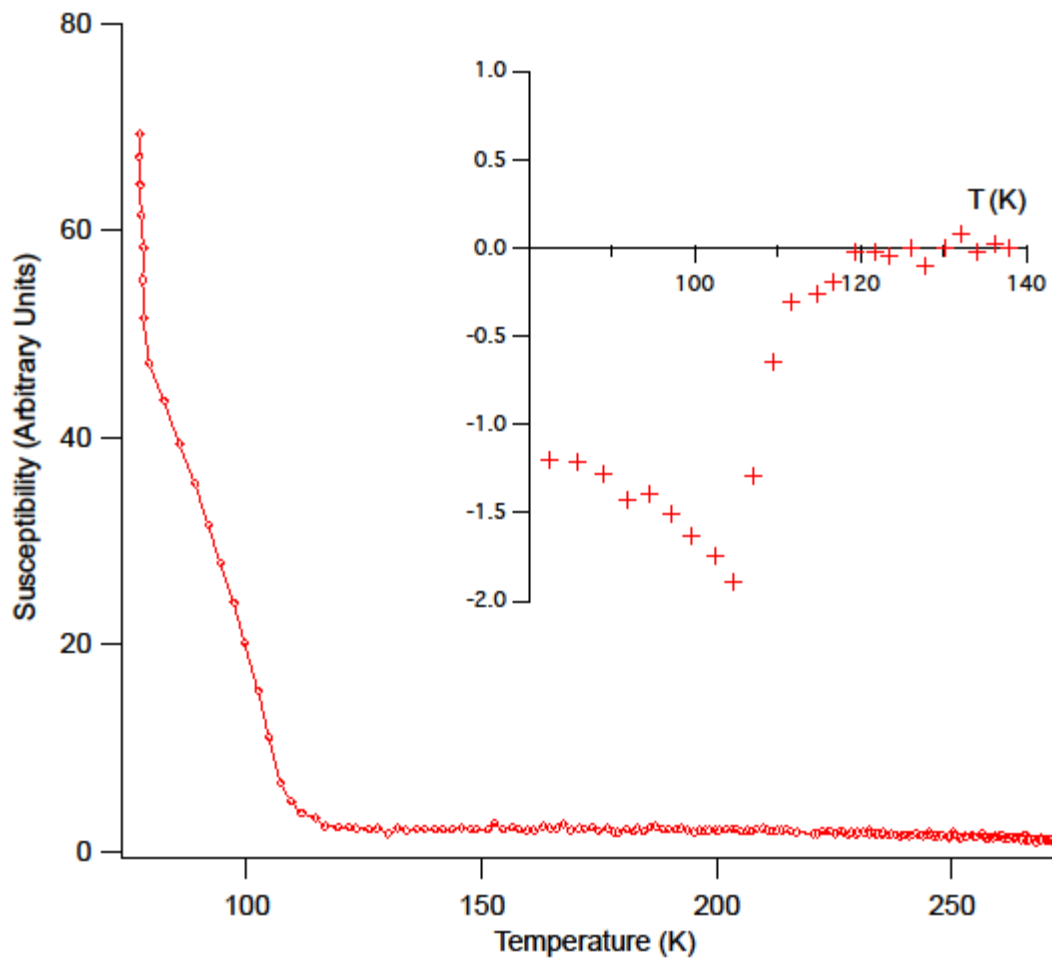
5

1
2
3



4
5
6
7
8

Fig. S10: X-ray diffractogram of a Fe₃O₄ reference material, the magnetic mesoparticles and theoretical diffraction peaks of Fe₃O₄ and NaCl, whereas NaCl occurs as a by-product during synthesis.



1
2
3
4
5

Fig. S11: Susceptibility as a function of temperature during warming from low temperature.

1 **Description of supplementary videos**

2 “Posfai_magnetite_mesocrystal_1”: tomographic tilt series of 3 aligned crystals

3 “Posfai_magnetite_mesocrystal_2”: tomographic tilt series of 2 individual crystals

4 “Posfai_mesocrystal1”: 3D reconstruction of data from “Posfai_magnetite_mesocrystal_1”

5 “Posfai_mesocrystal2”: 3D reconstruction of data from “Posfai_magnetite_mesocrystal_2”

6